

The particle size influence on crystallization kinetics of $(\text{GeS}_2)_{0.1}(\text{Sb}_2\text{S}_3)_{0.9}$ glass

P. Pustková^{a,*}, Z. Zmrhalová^b, J. Málek^b

^a Department of Inorganic Technology, University of Pardubice, Cs. legii sq. 565, 53210 Pardubice, Czech Republic

^b Department of Physical Chemistry, University of Pardubice, Cs. legii sq. 565, 53210 Pardubice, Czech Republic

Received 29 May 2007; received in revised form 18 August 2007; accepted 15 October 2007

Available online 23 October 2007

Abstract

The dependence of crystallization process on the particle size was studied for the pseudobinary chalcogenide glass $(\text{GeS}_2)_{0.1}(\text{Sb}_2\text{S}_3)_{0.9}$. Crystallization of Sb_2S_3 component was studied under isothermal and non-isothermal conditions using DSC. The strong dependence of crystallization process on the particle size was observed. With the increase of particle size the crystallization temperature range shifts to higher temperatures. This was observed for both isothermal and non-isothermal conditions. The activation energy of the process is for isothermal experiments higher than for non-isothermal experiments. The crystallization process was for all the samples described using autocatalytical model. Corresponding kinetic parameters are for crystallization under isothermal conditions lower than for non-isothermal crystallization.

© 2007 Elsevier B.V. All rights reserved.

Keywords: Crystallization; Kinetics; Chalcogenides; Glass; Particle size; Autocatalytical model

1. Introduction

Influence of the particle size of amorphous material on devitrification process was studied by several authors, the DSC (differential scanning calorimetry) or DTA (differential thermal analysis) techniques appear to be very suitable for this task. The results are published for silicate glasses [1–6], fluoride glasses [7–10], borate glasses [11,12], phosphate glasses [13], glasses containing waste material [14,15] and also chalcogenide glasses [16–18]. In most cases was the crystallization process studied under non-isothermal conditions and only several works report no influence on the temperature range position, size or shape of the crystallization peak [1,3,7,16–19]. The majority of reported crystallization data were strongly influenced by particle size of original (amorphous) material. The temperature shift of the crystallization peak for changing particle size is interpreted as a consequence of differences in heat transfer conditions as well as due to different number of nuclei. This is a plausible interpretation in the case when the peak is shifted to the higher temperatures with increasing particle size [1,10,11,13,20–23]

but also the non-systematic shift in temperature with increasing particle size was observed [2,9,14,24], even more complicated behavior was reported for some glass [25]. In some systems crystallization processes for which the peak position in temperature is not dependent on particle size can be observed, there is virtually no shift [1,3,7,16–19]. But in all these published results the crystallization peak was shifted to higher temperatures with increasing heating rate. The kinetic analysis of studied crystallization processes shows that the activation energy of crystallization processes E can be correlated to the particle size of origin amorphous material. Several reports show that there is no difference in the value of activation energy for different particle size [4,10,18,20] (the changes are about 1% related to the minimum reported value of E for individual published results). More reports can be found where E increases with increasing particle size [3,6,9,26] (the increase is from 7% to 15% related to the minimum value of E for individual published results) as well as there are many results where activation energy decreases with increasing particle size [2,5,7,8,12,15,21,24] (the decrease is from 7% to 290% related to the minimum values of E for individual published results). In some systems obvious minimum or maximum in the particle size dependence of E was observed [11,25]. On the basis of all these published results no conclusion can be made that for some class of glasses (silicate,

* Corresponding author. Tel.: +420 466 037 179; fax: +420 466 037 068.
E-mail address: pavla.pustkova@upce.cz (P. Pustková).

phosphate, fluoride, borate, etc.) is the dependence of crystallization peak temperature or activation energy on particle size shifted to higher or lower values.

This work contributes to the published results on the influence of the particle size of amorphous material on the crystallization process. A simple pseudobinary chalcogenide system $(\text{GeS}_2)_{0.1}(\text{Sb}_2\text{S}_3)_{0.9}$ was chosen. It has been reported [16] that for system As–Sb–Se the particle size of glass has no influence on the crystallization peak shape and its position in temperature scale. The same result was observed for glasses of composition As_2SeTe_2 [17] and As_2Se_3 [18]. But our previous data on crystallization in the $(\text{GeS}_2)_{0.2}(\text{Sb}_2\text{S}_3)_{0.8}$ glass showed that not only the peak position in temperature scale is changing with particle size but also change the value of activation energy and the kinetic parameters describing observed crystallization [27]. The difference in kinetic parameters between crystallization of bulk and powder sample was published also for the $(\text{GeS}_2)_{0.3}(\text{Sb}_2\text{S}_3)_{0.7}$ glass [28].

2. Kinetic analysis

The DSC is a very common technique for studying several processes. The kinetic equation of DSC curve can be described [29] as:

$$\Phi = \Delta HA e^{-E/RT} f(\alpha) \quad (1)$$

where Φ is the heat flow, ΔH the enthalpy change of the process, A the pre-exponential factor, E the activation energy of the process, R the universal gas constant, T the temperature, $f(\alpha)$ the kinetic model and α is the conversion. The kinetic analysis was made and the model acceptable for description of crystallization process was found using the characteristic functions $y(\alpha)$ and $z(\alpha)$ [28,30] defined as follows:

- under non-isothermal conditions

$$y(\alpha) = \Phi e^{E/RT} \quad (2)$$

$$z(\alpha) = \Phi T^2 \quad (3)$$

- under isothermal conditions

$$y(\alpha) = \Phi \quad (4)$$

$$z(\alpha) = \Phi t \quad (5)$$

where t is the time, other symbols are defined above. For the practical reasons are the both functions normalized within the (0, 1) range. The shape of characteristic functions and the conversion corresponding to the maximum of the functions, α_M for $y(\alpha)$ and α_p^{inf} for $z(\alpha)$, can be used to select the kinetic model suitable for description of the studied process. In the case of chalcogenide glasses the crystallization can usually be described by using the nucleation-growth model JMA(n)—Eq. (6), or by the autocatalytical model AC(M, N) [29]—Eq. (7).

$$f(\alpha) = n(1 - \alpha)[- \ln(1 - \alpha)]^{1-1/n} \quad (6)$$

$$f(\alpha) = \alpha^M(1 - \alpha)^N \quad (7)$$

The activation energy of the studied process is needed to calculate the characteristic functions and do the kinetic analysis. It is believed that the value of E can be calculated without any knowledge of the process mechanism although this approach was criticised [21,31,32]. But while the value of E may depend on the method, significant comparison may be achieved when using the same formula for evaluation [29]. The value of E for both isothermal and non-isothermal conditions can be calculated using the isoconversional method [33] where the slope of $\ln \Phi_\alpha$ dependence on $1/T_\alpha$ for the constant conversion corresponds to $-E/R$. The obtained value of E should not dependent on conversion for the α range (0.3, 0.7). The most frequently used method of E evaluation—the Kissinger method [34] is applicable only for non-isothermal experiments where the temperature corresponding to the maximum of peak T_p shifts with the heating rate β . The slope of the $\ln(\beta/T_p^2)$ dependence on $1/T_p$ is equal to the $-E/R$. Very similar is the Ozawa method [35] where the slope of the $\ln(\beta)$ dependence on $1/T_p$ is equal to $-1.052E/R$.

The parameter n of JMA model can be calculated from the dependence of $\ln[-\ln(1 - \alpha)]$ on $\ln(t)$ or $1/T$ for isothermal and non-isothermal conditions, respectively [28]. The conversion corresponding to the maximum of $y(\alpha)$ function can be also used to determine the parameter n [28] as $n = 1/[1 + \ln(1 - \alpha_M)]$. Conversion α_M can be also used to determine the parameters of AC model, because $M/N = \alpha_M/(1 - \alpha_M)$. When is known the activation energy of the process and the conversion ratio then the parameters of AC model and pre-exponential factor A can be determined from the dependence [36]:

$$\ln \left[\Phi \exp \left(\frac{E}{RT} \right) \right] = \ln(\Delta HA) + N \ln[\alpha^{M/N}(1 - \alpha)] \quad (8)$$

3. Experimental

The pseudobinary glass $(\text{GeS}_2)_{0.1}(\text{Sb}_2\text{S}_3)_{0.9}$ was prepared from pure elements. The adequate amounts of elements were weighted into the quartz ampoule. The ampoule was then evacuated, sealed and put into the rocking furnace. The batched ampoule was heated at 950 °C for 20 h. The amorphous material was obtained when the ampoule was quickly pushed from the furnace into the bath with water and ice. The amorphous character of the prepared glass was confirmed by X-ray diffraction. The crystallization of Sb_2S_3 in $(\text{GeS}_2)_{0.1}(\text{Sb}_2\text{S}_3)_{0.9}$ glassy matrix was studied. The X-ray diffraction confirmed that the crystalline form is Sb_2S_3 (stibnite) and the results of as prepared and crystallized $(\text{GeS}_2)_{0.1}(\text{Sb}_2\text{S}_3)_{0.9}$ sample is shown in Fig. 1. The crystallization measurements were performed on samples in the form of bulk and powder to prove the influence of surface/volume ratio on crystallization process. Bulk samples were prepared as thin plates (thickness 0.85 mm) both side polished to the optical quality with the maximum sample dimension 3 mm (to be able to be put in DSC crucible). The pieces of glass were crushed to the powder which was divided according to the particle size into eight fractions: under 0.02, 0.02–0.05, 0.05–0.125, 0.125–0.18, 0.18–0.25, 0.25–0.3, 0.3–0.5 and 0.5–0.8 mm. The average particle size d_{aver} of each fraction (0.01, 0.035, 0.0875, 0.1525, 0.215, 0.275, 0.4 and 0.65 mm, respectively) was used

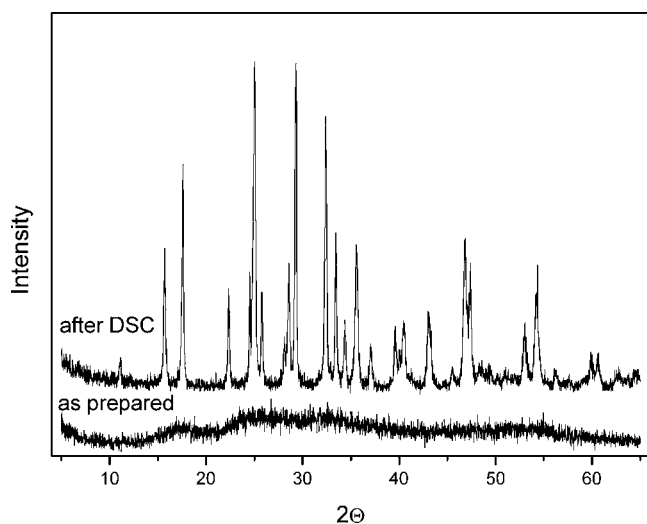


Fig. 1. X-ray diffraction pattern of as prepared and crystallized $(\text{GeS}_2)_{0.1}(\text{Sb}_2\text{S}_3)_{0.9}$ glass.

when plotting and analyzing the DSC data as a function of particle size, for the bulk sample is used the value 3 mm. The powder fractions were prepared (from the very breaking of the quartz ampoule till the weighting of sample into the DSC crucibles) under the protective atmosphere of argon and stored in a desiccator under argon atmosphere until used for the DSC measurement. The influence of oxygen on the studied crystallization process was tested when the powder with 0.02–0.05 mm particle size was prepared also without the protective atmosphere (on air). The crystallization of Sb_2S_3 in $(\text{GeS}_2)_{0.1}(\text{Sb}_2\text{S}_3)_{0.9}$ glassy matrix was studied under isothermal and non-isothermal conditions using DSC Pyris 1 (measurements were done in the atmosphere of nitrogen). No pre-nucleation treatment has been used. All samples (bulk and each fraction of powder sample) were heated from 100 to 380 °C with heating rates 2, 5, 7, 10, 15, 20 and 30 K min^{-1} . The temperature of isothermal experiments and the time of the isotherm were different for each particle size. Generally, during isothermal experiments the isotherm temperature was in the range 266–310 °C and the time needed for crystallization ranged between 6 and 80 min. The temperature range of isotherms was selected on the base of the crystallization rate for each particle size. Below the minimum temperature the rate was too slow and that above the maximum temperature was too fast (crystallization started within few seconds after the sample reached the isotherm temperature) to produce a reasonable peak shape for experimental data analysis. The sample was heated to the temperature of isotherm with heating rate 150 K min^{-1} . The sample mass for the DSC experiments was ca. 20 mg for bulk sample and 12 mg for powder sample.

4. Results

The crystallization of Sb_2S_3 in pseudobinary $(\text{GeS}_2)_{0.1}(\text{Sb}_2\text{S}_3)_{0.9}$ glass was studied under isothermal and non-isothermal conditions. The main attention is focused on the

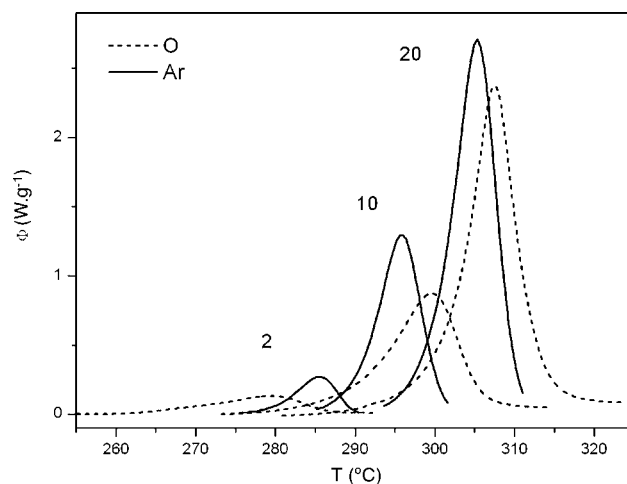


Fig. 2. The influence of surrounding atmosphere during preparation of powder samples on the consequent crystallization. The DSC results for sample prepared under protective atmosphere (Ar) and without it (O) are presented for heating rates 2, 10 and 20 K min^{-1} .

particle size influence to crystallization behavior and its kinetic description.

The powder samples of $(\text{GeS}_2)_{0.1}(\text{Sb}_2\text{S}_3)_{0.9}$ glass were prepared under the protective atmosphere to prevent them from adsorbing oxygen which would influence the studied crystallization process. The fraction with 0.02–0.05 mm particle size was prepared also without the protective atmosphere and the non-isothermal measurements were performed. The comparison of crystallization peaks is for both samples and various heating rates shown in Fig. 2. The enthalpy change of crystallization is -55.0 ± 2.2 and $-52.7 \pm 2.2 \text{ J g}^{-1}$ for powder prepared without and under the protective atmosphere, respectively. Within error limits is the value for both samples the same. But it is clear that the crystallization process may be quite different—the peak for sample prepared under argon atmosphere is higher and narrower than that for the sample prepared without the protective atmosphere. More complicated crystallization process in the case of the sample prepared without the protective atmosphere can be deduced from the shape of the DSC peak and even better from the $y(\alpha)$ and $z(\alpha)$ functions, especially for heating rate 2 K min^{-1} . The difference is probably caused by the oxygen presence on the surface of the sample prepared on air. One could suppose that oxygen increases the number of nuclei on the surface so the crystallization process should be faster and observed at lower temperature compared to the sample prepared under Ar atmosphere. But as can be seen in Fig. 2 this is not the case. Živković et al. [37] studied the influence of oxygen on crystalline Sb_2S_3 and observed two exothermic effects in temperature range 283–478 and 595–610 °C. Authors predicated them to the transformation of Sb_2S_3 to SbO_2 . The temperature range of the first observed effect overlaps the region of Sb_2S_3 crystallization in $(\text{GeS}_2)_{0.1}(\text{Sb}_2\text{S}_3)_{0.9}$ glass and may influence the observed process. Therefore, all the powder samples were prepared under the protective atmosphere of argon to prevent possible influence of oxygen on observed crystallization process. The surface/volume ratio in

Table 1
The values of the enthalpy change ΔH during isothermal (iso) and non-isothermal (non-iso) crystallization and of its activation energy (kJ mol^{-1}) determined by isoconversional, Kissinger and Ozawa method for bulk and powder samples with different particle size

Sample (mm)	$-\Delta H$ (J g^{-1})		Isoconversional		Kissinger	Ozawa
	Iso	Non-iso	Iso	Non-iso		
Bulk	50.2 ± 4.4	61.9 ± 1.3	280 ± 30	279 ± 8	253 ± 5	251 ± 5
0.5–0.8	59.0 ± 0.6	61.1 ± 1.8	277 ± 11	275 ± 21	260 ± 8	256 ± 7
0.3–0.5	57.7 ± 1.3	60.1 ± 1.9	292 ± 2	271 ± 9	266 ± 4	262 ± 3
0.25–0.3	58.3 ± 1.4	59.4 ± 3.0	289 ± 3	286 ± 13	264 ± 8	260 ± 8
0.18–0.25	56.8 ± 0.2	57.3 ± 2.3	300 ± 2	287 ± 10	260 ± 5	256 ± 4
0.125–0.18	55.3 ± 1.2	57.0 ± 2.3	302 ± 4	268 ± 9	241 ± 9	238 ± 8
0.05–0.125	54.9 ± 0.6	57.2 ± 1.9	304 ± 3	291 ± 13	266 ± 11	262 ± 11
0.02–0.05	52.7 ± 1.3	56.3 ± 1.5	304 ± 3	340 ± 36	309 ± 26	303 ± 25
Under 0.02	52.9 ± 0.6	54.6 ± 1.4	310 ± 4	369 ± 57	311 ± 7	305 ± 6

bulk samples was not so high compared to powder samples, so the bulk samples were prepared without the protective atmosphere.

The crystallization of Sb_2S_3 in our glass was under non-isothermal conditions observed in the temperature range $270\text{--}345^\circ\text{C}$ for all studied samples and all heating rates. The temperatures of isotherms were approximately in the temperature range where the crystallization for heating rate 2 K min^{-1} was observed for the corresponding particle size. The values of enthalpy change of crystallization are summarized in Table 1. The variation of ΔH with particle size under both isothermal and non-isothermal conditions is shown in Fig. 3. The value of ΔH increases with increasing particle size but for bulk sample measured under isothermal conditions is the enthalpy change almost the same as that for the finest powders.

The samples were after the DSC measurement examined by optical microscope (Fig. 4). The samples for the particle size from under 0.02 mm to 0.05–0.125 mm were compact having the shape of the DSC crucible. For larger particle size up to 0.3–0.5 mm the sample also imitated the crucible shape but the mass was less compact with the free space increas-

ing with increasing particle size. The sample with particle size 0.5–0.8 mm remained in the form of separate pieces—even after the crystallization. The crystals similar to that published by Švadlák et al. [38] (Fig. 5A in their work) for the $(\text{GeS}_2)_{0.2}(\text{Sb}_2\text{S}_3)_{0.8}$ glass were observed at the surface of the fully crystallized sample.

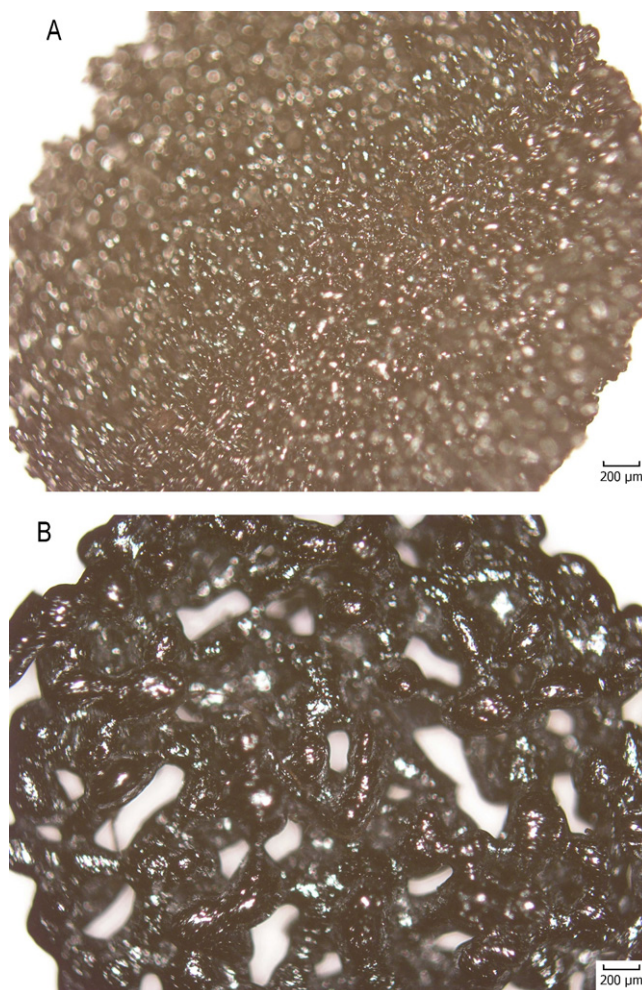


Fig. 4. Samples after isothermal DSC experiment for the particle size: (A) 0.05–0.125 mm and (B) 0.25–0.3 mm.

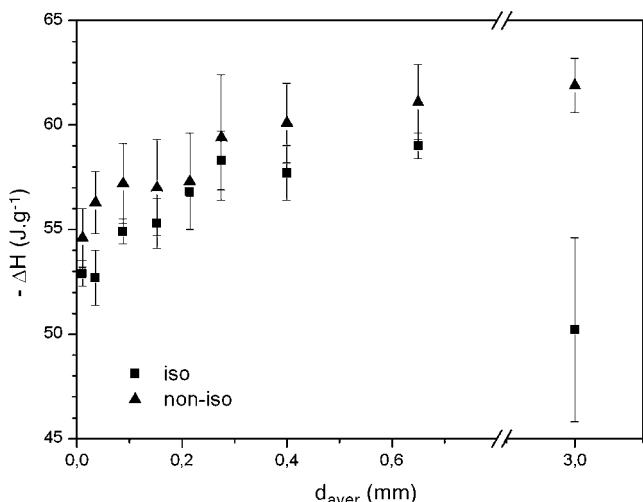


Fig. 3. The particle size dependence of crystallization enthalpy change for isothermal and non-isothermal conditions.

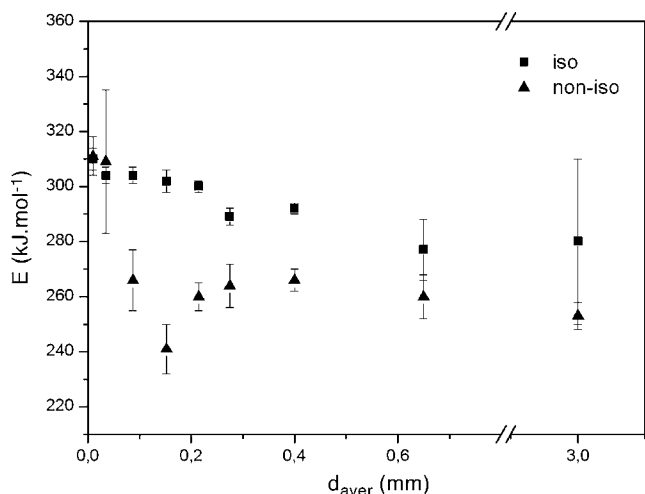


Fig. 5. The particle size dependence of activation energy of the crystallization process determined for isothermal (isoconversional method) and non-isothermal (Kissinger method) conditions.

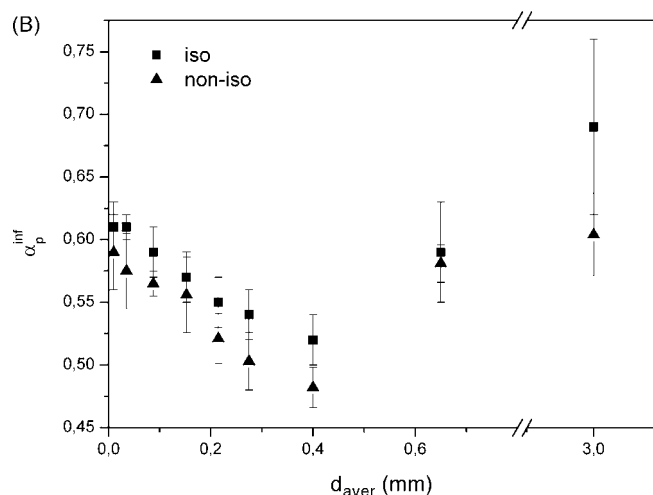
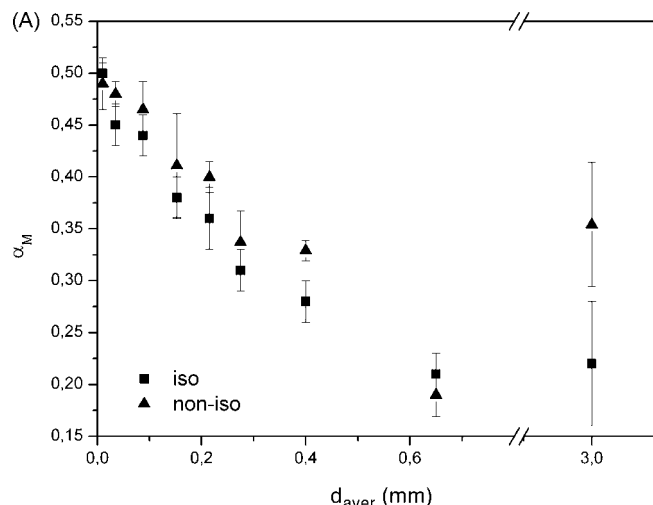


Fig. 7. The particle size dependence of the conversion corresponding to the maximum of $y(\alpha)$ and $z(\alpha)$ functions (α_M and α_p^{inf}) for crystallization under isothermal and non-isothermal conditions.

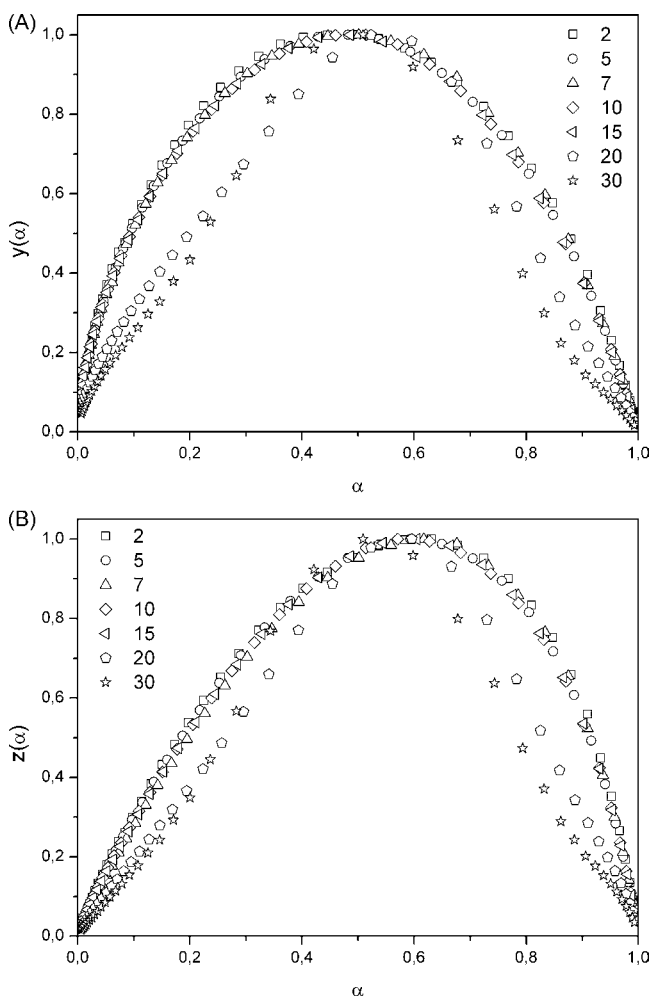


Fig. 6. Characteristic functions $y(\alpha)$ and $z(\alpha)$ for non-isothermal crystallization of powder with particle size under 0.02 mm.

5. Discussion

The crystallization of Sb_2S_3 in pseudobinary $(GeS_2)_{0.1}(Sb_2S_3)_{0.9}$ glass was studied by DSC under isothermal and non-isothermal conditions with samples in the form of the bulk and of the powder divided into eight fractions according to the particle size. In most glasses the crystallization proceeds by internal and surface mechanisms simultaneously and competitively [22]. Our aim was to clarify if in the case of chalcogenide $GeS_2-Sb_2S_3$ glass both these mechanisms are equivalent for both fine powder and bulk. Isothermal and non-isothermal experiments were performed for all the samples to compare the potential differences. It is believed that the techniques of isothermal analysis are in most cases more definite though the non-isothermal thermoanalytical techniques have several advantages (faster proceeding, wider temperature range compared to the isothermal experiments) [39].

The illustration of the DSC curves for isothermal and non-isothermal crystallization and selected particle sizes is shown in Fig. 10. As can be seen for non-isothermal crystallization the temperature of the peak maximum is shifted to higher tempera-

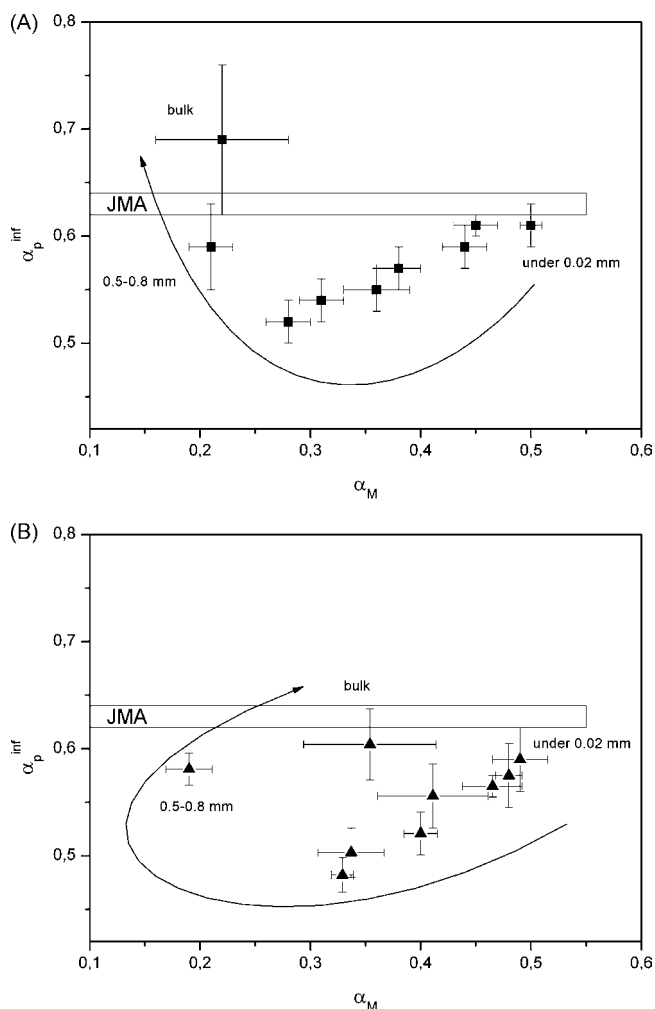


Fig. 8. The dependence of the conversion α_p^{inf} on α_M for (A) isothermal and (B) non-isothermal conditions. The area of JMA model applicability is suggested. The solid curves guide the eye in direction of change from the fraction under 0.02 mm to the bulk sample.

tures with higher heating rates. For each heating rate the T_p value increases with increasing particle size. Up to the 0.05–0.125 mm fraction the increase is higher than for the other (larger) particle sizes. One explanation of the T_p shift with particle size can be that the crushing of the bulk to the powder can influence the subsequent crystallization process. There are some reports on the mechanical treatment influence on the crystallization behavior [40,41] but usually an intensive ball-milling was applied. Thornburg [17] observed no significant influence of powder sample preparation by crushing on the crystallization process in As_2SeTe_2 glass. The dependence of T_p on the particle size has almost the same trend for all used heating rates. The difference in T_p between bulk and particle size below 0.02 mm is 25, 28 and 32 °C for heating rates 2, 10 and 30 K min^{-1} , respectively. This probably means that even during slow heating, the number of nuclei in the sample is not very different compared to high-heating rates. It appears that the sample was nucleated (whether on the surface or volume) before any heating treatment was applied. In the case that the sample was fully nucleated before inserting in DSC the T_p shift with particle size would

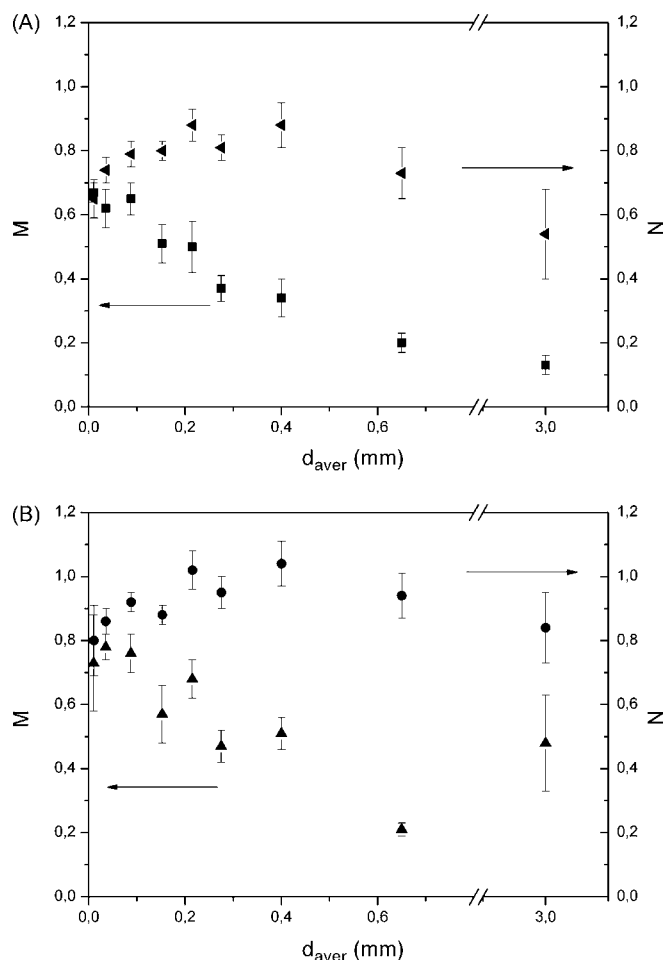


Fig. 9. The particle size dependence of parameters M and N of the autocatalytical model describing the crystallization process for (A) isothermal and (B) non-isothermal conditions.

not be so high. The dominant mechanism of crystallization (surface or internal) was determined on the base of T_p dependence of particle size [1,11]. On the other hand, according to Ray et al. [22] this information is not sufficient to provide this interpretation (they observed that the value of T_p increased with the particle size whether the main crystallization mechanism was surface or internal). The shape of crystallization peaks for different particle sizes is shown in Fig. 10. It is published for non-isothermal experiments that the sharp peak means that the internal crystallization is dominant and broad peak signals the dominant surface crystallization [22,24]. This is opposite to our own results. The surface/volume ratio decreases with increasing particle size. Therefore, the surface mechanism should more influence the small particles where the crystallization peak is sharp compared to larger particle size. The interpretation of peak shape and dominant crystallization mechanism has been proposed for silicate glasses but it seems to be not valid for chalcogenide glass. The particle size dependence of the activation energy can be used to estimate the mechanism of the studied process.

It is believed that the value of activation energy E can be calculated without any other information about the crystallization mechanism although some authors have still some doubts about

Table 2

The parameters M and N of the autocatalytical model and values of pre-exponential factor describing the isothermal (iso) and non-isothermal (non-iso) crystallization for bulk and powder samples with different particle size

Sample (mm)	M		N		$\ln(A) (s^{-1})$	
	Iso	Non-iso	Iso	Non-iso	Iso	Non-iso
Bulk	0.13 ± 0.03	0.48 ± 0.15	0.54 ± 0.14	0.84 ± 0.11	52.5 ± 0.2	47.7 ± 0.2
0.5–0.8	0.20 ± 0.03	0.21 ± 0.02	0.73 ± 0.08	0.94 ± 0.07	53.0 ± 0.1	49.5 ± 0.1
0.3–0.5	0.34 ± 0.06	0.51 ± 0.05	0.88 ± 0.07	1.04 ± 0.07	56.9 ± 0.1	51.7 ± 0.1
0.25–0.3	0.37 ± 0.04	0.47 ± 0.05	0.81 ± 0.04	0.95 ± 0.05	56.5 ± 0.1	51.5 ± 0.1
0.18–0.25	0.50 ± 0.08	0.68 ± 0.06	0.88 ± 0.05	1.02 ± 0.06	59.3 ± 0.1	51.1 ± 0.1
0.125–0.18	0.51 ± 0.06	0.57 ± 0.09	0.80 ± 0.03	0.88 ± 0.03	59.9 ± 0.1	47.2 ± 0.1
0.05–0.125	0.65 ± 0.05	0.76 ± 0.06	0.79 ± 0.04	0.92 ± 0.03	60.6 ± 0.1	52.9 ± 0.1
0.02–0.05	0.62 ± 0.06	0.78 ± 0.04	0.74 ± 0.04	0.86 ± 0.04	61.2 ± 0.1	62.6 ± 0.2
Under 0.02	0.67 ± 0.03	0.73 ± 0.15	0.65 ± 0.06	0.80 ± 0.11	62.9 ± 0.1	63.6 ± 0.2

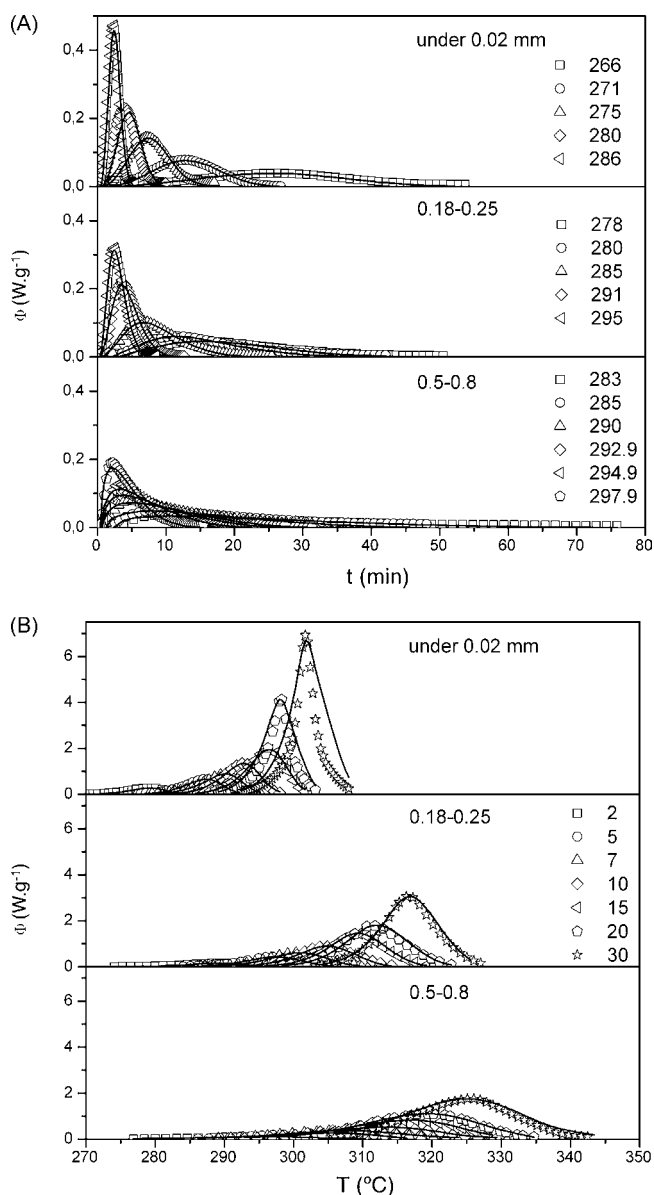


Fig. 10. Experimental (points) and calculated (lines) data for (A) isothermal and (B) non-isothermal crystallization and particle sizes (from top to bottom): under 0.02, 0.18–0.25 and 0.5–0.8 mm. The temperatures of isotherms ($^{\circ}\text{C}$) and heating rates (K min^{-1}) are inserted. The lines are calculated for parameters summarized in Table 2.

this presumption [10,21]. The value of E can be determined from the crystallization exotherm measured either isothermally or non-isothermally. Several thermoanalytical methods [29,32] have been used to analyze the non-isothermal crystallization data but all these methods based on the formal theory of isothermal transformation kinetics [29]. Despite the criticism the non-isothermal experiments are preferred over the isothermal experiments and are frequently used to study the crystallization kinetics of glasses. The reason is that the non-isothermal experiments are less time consuming and the analysis of experimental data is less complicated. The values of E for non-isothermal crystallization were calculated according to the Kissinger and Ozawa methods [34,35] and are summarized in Table 1. For both these methods the obtained values for non-isothermal crystallization are very close with low error limits—with the exception of the 0.02–0.05 mm fraction. The activation energy of the process for isothermal and non-isothermal conditions can be calculated by the isoconversional method. These values of E (Table 1) for both isothermal and non-isothermal crystallization are close for bulk and larger particle size. But for smaller particle sizes and non-isothermal conditions the calculated value of E strongly depended on the conversion so the isoconversional method should not be used for these fractions. That is why we used the value of E calculated by isoconversional method for isothermal crystallization and values calculated by Kissinger method for non-isothermal crystallization in our further kinetic analysis. These values of E and their dependence on particle size are illustrated in Fig. 5. For the isothermal crystallization the activation energy slightly decreases with increasing particle size and for 0.5–0.8 mm and bulk is already similar. In the case of non-isothermal crystallization there is a minimum of E present at the 0.125–0.18 mm fraction and then for larger particle size the value of E remains similar. It can be found in literatures that the values of E determined using non-isothermal DSC or DTA experiments are close to the activation energy of the crystal growth E_G [2,9] or activation energy of viscous flow E_{η} [10,21,23]. For chalcogenide As_2Se_3 glass Henderson and Ast [18] found that E_{η} is close to the activation energy of nucleation E_N . For $(\text{GeS}_2)_{0.1}(\text{Sb}_2\text{S}_3)_{0.9}$ glass the viscosity measurements and direct measurement of crystal growth were performed. The value of activation energy of crystal growth was determined as $E_G = 405 \pm 7 \text{ kJ mol}^{-1}$ [42]. The activation energy of vis-

cous flow is $E_\eta = 513 \pm 8 \text{ kJ mol}^{-1}$ measured in the temperature range 207–259 °C [43]. In comparison with the activation energy for the bulk sample are both these values significantly higher. The value of E for bulk sample and crystallization studied under non-isothermal conditions can be for $(\text{GeS}_2)_{0.1}(\text{Sb}_2\text{S}_3)_{0.9}$ glass compared with composition $(\text{GeS}_2)_{0.2}(\text{Sb}_2\text{S}_3)_{0.8}$ [27] and $(\text{GeS}_2)_{0.3}(\text{Sb}_2\text{S}_3)_{0.7}$ [28]. The value of activation energy is for $(\text{GeS}_2)_{0.1}(\text{Sb}_2\text{S}_3)_{0.9}$ glass higher than for the other compositions as well as are the values of E_G and E_η [42,43].

The suitable kinetic model for description of the studied process was chosen on the base of the characteristic functions $y(\alpha)$ and $z(\alpha)$ which were calculated from experimental data according to Eqs. (2)–(5). The illustration of the shape of these functions is depicted in Fig. 6 for non-isothermal crystallization. Shape of both these functions is the same for lower heating rates but is different for heating rates 20 and 30 K min⁻¹. This means that the mechanism of the process is changed for these high-heating rates. As the particle size increases the difference between lower and higher heating rates slightly decreases but with increasing particle size increases the dispersion of the curves for the appropriate size (the curves do not overlap in the whole range of conversion). In the case of isothermal crystallization is the shape of both characteristic functions the same for all isotherm temperatures for each particle size but there also occurs increase of the dispersion of the curves with increasing particle size. The curvature of $y(\alpha)$ function is more asymmetric with increasing particle size and conversion corresponding to the maximum of this function is also apparently shifted with increasing particle size for both isothermal and non-isothermal crystallization. In the case of function $z(\alpha)$ there is also shift in the conversion corresponding to the maximum of this function but it is not so large and the function itself is also not so asymmetric. The particle size dependence of the conversion corresponding to the maximum of both characteristic functions for isothermal and non-isothermal crystallization is shown in Fig. 7. Decrease of the α_M and α_p^{inf} values can be observed with increasing particle size up to the 0.5–0.8 and 0.3–0.5 mm fraction, respectively, then for larger particle sizes the values increase again. This dependence on particle size is the same for isothermal and non-isothermal crystallization. This could imply some changes of the crystallization mechanism but for both characteristic functions the change occurs at slightly different particle sizes. The correspondence of α_M and α_p^{inf} changes with particle size for both isothermal and non-isothermal data implies that using non-isothermal measurements of crystallization do not change the α_M and α_p^{inf} values significantly. This is important because the values α_M and α_p^{inf} can be used to determinate the kinetic model suitable for description of experimental data [30]. The dependence of α_p^{inf} on α_M is shown in Fig. 8 where the range of JMA model applicability is suggested. From this dependence it is evident that for both isothermal and non-isothermal crystallization is the crystallization process different for 0.5–0.8 mm powder and bulk compared to smaller particle sizes. Testing the acceptability of kinetic model showed that for the sample in the form of powder JMA model should not be used, the bulk samples are within the error limit close to the range of JMA model applicability. In the case of isothermal crystallization the 0.5–0.8 mm

fraction seems to contain particles large enough to correlate with the bulk sample as well as description using JMA model. This is not observed for non-isothermal conditions where the bulk and 0.5–0.8 mm powder differ significantly. In this case can be reflected the difference in heat transfer which has no significant influence when the crystallization is studied under isothermal conditions. The conversion corresponding to the maximum of characteristic functions fulfils the condition that $0 < \alpha_M < \alpha_p^{\text{inf}}$ so the AC model can be used to describe the observed crystallization. The crystallization process was for all the studied samples described by AC model (though the JMA model was applicable for the bulk sample) to provide the possibility to correlate the particle size influence on AC model parameters. The value of α_M is used to calculate the quotient of the parameters of AC model and then the parameters can be calculated according to Eq. (8). The value of pre-exponential factor A was recalculated to give the best fit of experimental data. The values of AC parameters and pre-exponential factor for isothermal and non-isothermal conditions and different particle sizes are summarized in Table 2. The particle size influence on values of parameter M and N for isothermal and non-isothermal conditions is shown in Fig. 9. The illustration of the calculated lines (for parameters in Table 2) correspondence with the experimental data is depicted in Fig. 10 for selected powder fractions. The value of parameter M decreases with particle size while the parameter N increases with increasing particle size up to 0.3–0.5 mm fraction and then decreases for both isothermal and non-isothermal data.

To conclude, from results based mainly on isothermal experiments we can induce that the values of E , α_M and α_p^{inf} are changing with particle size in the whole range of particle sizes. Therefore, the surface mechanism of crystallization is probably dominant for all sizes. The particles with 0.5–0.8 mm size seem to be big enough and are practically corresponding to the bulk sample under isothermal conditions.

6. Conclusions

The crystallization of Sb_2S_3 in the $(\text{GeS}_2)_{0.1}(\text{Sb}_2\text{S}_3)_{0.9}$ glass was studied under isothermal and non-isothermal conditions. Main interest was focused on the glass particle size influence on crystallization process and its kinetic description. With the increasing particle size of amorphous material are the crystallization effects shifted to higher temperatures. The values of activation energy and conversions corresponding to the maximum of characteristic functions are changing in the whole range of particle sizes. That probably means that the surface mechanism is the most significant one in the case of Sb_2S_3 crystallization in the $(\text{GeS}_2)_{0.1}(\text{Sb}_2\text{S}_3)_{0.9}$ glass.

Acknowledgement

This work was supported by the project MSM 0021627501 from the Ministry of Education, Youth and Sports of the Czech Republic.

References

- [1] P. Loiseau, D. Caurant, O. Majerus, N. Baffier, C. Fillet, *J. Mater. Sci.* 38 (2003) 853–864.
- [2] N. Koga, J. Šesták, Z. Strnad, *Thermochim. Acta* 203 (1992) 361–372.
- [3] S. Likitranichkul, W.C. Lacourse, *J. Mater. Sci.* 33 (1998) 5901–5904.
- [4] I.W. Donald, *J. Mater. Sci.* 30 (1995) 904–915.
- [5] A. Marotta, A. Buri, F. Branda, *Thermochim. Acta* 40 (1980) 397–403.
- [6] Y. Hu, C.-L. Huang, *J. Non-Cryst. Solids* 278 (2000) 170–177.
- [7] A. Ozturk, *Phys. Chem. Glasses* 41 (2000) 71–74.
- [8] B.J. Costa, M. Poulain, Y. Messaddeq, S.J.L. Ribeiro, *J. Non-Cryst. Solids* 273 (2000) 76–80.
- [9] M.B. Tošić, R.Ž. Dimitrijević, M.M. Mitrović, *J. Mater. Sci.* 37 (2002) 2293–2303.
- [10] D.R. Macfarlane, M. Matecki, M. Poulain, *J. Non-Cryst. Solids* 64 (1984) 351–362.
- [11] X. Xie, H. Gao, *J. Non-Cryst. Solids* 240 (1998) 166–176.
- [12] S.W. Lee, K.B. Shim, K.H. Auh, P. Knott, *J. Non-Cryst. Solids* 248 (1999) 127–136.
- [13] V.C.S. Reynoso, K. Yukimitu, T. Nagami, C.L. Carvalho, J.C.S. Moraes, E.B. Araújo, *J. Phys. Chem. Solids* 64 (2003) 27–30.
- [14] A.A. Francis, *Mater. Res. Bull.* 41 (2006) 1146–1154.
- [15] Y.J. Park, J. Heo, *Ceram. Int.* 28 (2002) 669–673.
- [16] S. Mahadevan, A. Giridhar, A.K. Singh, *J. Non-Cryst. Solids* 88 (1986) 11–34.
- [17] D.D. Thornburg, *Mater. Res. Bull.* 9 (1974) 1481–1486.
- [18] D.W. Henderson, D.G. Ast, *J. Non-Cryst. Solids* 64 (1984) 43–70.
- [19] T. Unyi, A. Juhász, P. Tasnádi, J. Lendvai, *J. Mater. Sci.* 35 (2000) 3059–3068.
- [20] W. Li, B.S. Mitchell, *J. Non-Cryst. Solids* 255 (1999) 199–207.
- [21] K. Matusita, S. Sakka, *J. Non-Cryst. Solids* 38–39 (1980) 741–746.
- [22] C.S. Ray, D.E. Day, *Thermochim. Acta* 280/281 (1996) 163–174.
- [23] J. Götz, *Phys. Chem. Glasses* 18 (1977) 32–35.
- [24] C.S. Ray, W. Huang, D.E. Day, *J. Am. Ceram. Soc.* 74 (1991) 60–66.
- [25] L. Kashif, A.A. Soliman, A.M. Sanad, *Phys. Chem. Glasses* 39 (1998) 195–199.
- [26] E. Idalgo, E.B. Araújo, K. Yukimitu, J.C.S. Moracs, V.C.S. Reynoso, C.L. Carvalho, *Mater. Sci. Eng. A* 434 (2006) 13–18.
- [27] P. Pustková, D. Švadlák, J. Shánělová, J. Málek, *Thermochim. Acta* 445 (2006) 116–120.
- [28] J. Málek, *Thermochim. Acta* 355 (2000) 239–253.
- [29] J. Šesták, *Thermophysical Properties of Solids, Their Measurements and Theoretical Analysis*, Elsevier, Amsterdam, 1984.
- [30] J. Málek, *Thermochim. Acta* 200 (1992) 257–269.
- [31] C.S. Ray, D.E. Day, W. Huang, K.L. Narayan, T.S. Cull, K.F. Kelton, *J. Non-Cryst. Solids* 204 (1996) 1–12.
- [32] H. Yinnon, D.R. Uhlmann, *J. Non-Cryst. Solids* 54 (1983) 253–275.
- [33] H.L. Friedman, *J. Polym. Sci. C6* (1964) 183–195.
- [34] H.E. Kissinger, *Anal. Chem.* 29 (1957) 1702–1706.
- [35] T. Ozawa, *J. Therm. Anal.* 2 (1970) 301–324.
- [36] J. Málek, *Sci. Papers Univ. Pardubice* 2 (1996) 177–208.
- [37] Z. Živković, N. Štrbac, D. Živković, D. Grujičić, B. Boyanov, *Thermochim. Acta* 383 (2002) 137–143.
- [38] D. Švadlák, P. Pustková, P. Košťál, J. Málek, *Thermochim. Acta* 446 (2006) 121–127.
- [39] D.W. Henderson, *J. Non-Cryst. Solids* 30 (1979) 301–315.
- [40] M. Ciecinska, *J. Therm. Anal. Calorim.* 84 (2006) 201–205.
- [41] J. Bednarcik, E. Burkel, K. Saksl, P. Kollar, S. Roth, *J. Appl. Phys.* 100 (2006) 014903.
- [42] J. Málek, D. Švadlák, P. Pustková, *Ninth European Symposium on Thermal Analysis and Calorimetry (Lecture)*, Kraków, Poland, 2006.
- [43] J. Shánělová, P. Košťál, J. Málek, *J. Non-Cryst. Solids* 352 (2006) 3952–3955.